

Geospatial Assessment of State Lands in the Cape Coast Urban Area

E. B. Quarcoo, I. Yakubu, K. J. Appau

Abstract—Current land use and land cover (LULC) dynamics in Ghana have revealed considerable changes in settlement spaces. As a result, this study is intended to merge the cellular automata and Markov chain models using remotely sensed data and Geographical Information System (GIS) approaches to monitor, map, and detect the spatio-temporal LULC change in state lands within Cape Coast Metropolis. Multi-temporal satellite images from 1986-2020 were pre-processed, geo-referenced, and then mapped using supervised maximum likelihood classification to investigate the state's land cover history (1986-2020) with an overall mapping accuracy of approximately 85%. The study further observed the rate of change for the area to have favored the built-up area 9.8 (12.58 km²) to the detriment of vegetation 5.14 (12.68 km²), but on average, 0.37 km² (91.43 acres, or 37.00 ha.) of the landscape was transformed yearly. Subsequently, the CA-Markov model was used to anticipate the potential LULC for the study area for 2030. According to the anticipated 2030 LULC map, the patterns of vegetation transitioning into built-up regions will continue over the following ten years as a result of urban growth.

Keywords—LULC, cellular automata, Markov Chain, state lands, urbanisation, public lands, cape coast metropolis.

I. INTRODUCTION

THE impact of urbanisation on the African continent is characterised by a bicephalic pattern of events where large African cities grow disproportionately large compared to other urban areas. In 2014, the UN further identified the African continent as moving swiftly into the “urban age,” though largely rural [1]. According to [1], the projected statistics on urbanisation for the continent for forty years (2010–2050) are expected to triple from 395 million to 1.33 billion, corresponding to 21% of the global projected urban population.

In 1960, the Ghanaian urban population stood at 23% and was projected to hit a 59.2% high by 2020 [2]. Characterised by socio-economic developments, urban areas attract more people increasing the general population [3]. A population increase is bound to mount pressure on both finite and infinite natural resources, of which land, a finite resource is the greatest of them all. This was further corroborated by [4] when they iterated that the basic microcosm for all forms of economic growth and national development is hinged on land. This forms the basis for why land must be managed to the benefit of both current and future generation's sustainability.

The considerable importance of land again requires prudent

management skills to effectively and efficiently manage it, as a reverse would result in associated dangers with urbanisation (sprawl effects, slums, congestion, pollution, and many more). The future generation's fate is determined based on predictive studies on LULC for the landscape under study, which are done based on tried and tested models proven to be reliable over the years.

Studies on LULC change are frequently employed to track changes in the environment brought forth by humans. Many studies have confirmed that complex anthropogenic-environmental interactions are the cause of land use and land cover change (LULCC) [5]. It is challenging to pinpoint the primary drivers of social-ecological systems due to their high levels of interdependency [6]. Land use planning, particularly in developing nations, must take into account the primary drivers of LULCCs, including indirect (underlying) variables that are difficult to identify through spatial or economic analysis.

The loss of forests and agricultural land in many exurban regions has been made worse by rising global urbanization, which has also raised poverty rates among smallholder farmers who practice subsistence farming [7]. Critical instruments for collecting precise and timely geographical data on LULC and assessing changes in a study region are Geographic Information Systems (GIS) and Remote Sensing (RS) [8].

To identify and monitor land uses at different scales, RS pictures record LULC conditions with ease and provide an abundance of data from which current LULC information and changes may be effectively retrieved, analysed, and simulated [9]. That being said, GIS offers a flexible environment for collecting, archiving, displaying, and evaluating the digital data needed for change detection [10].

While there are several techniques for identifying and analysing LULC changes, the analysis of historical remotely sensed images using RS and GIS technologies enables effective monitoring and forecasting of LULC change patterns. This might provide a framework for methodical and efficient management, planning, and restoration of land used for socioeconomic development [11]. Numerous methods for predicting LULC changes are easily found in the literature. These methods vary in terms of their objectives, protocols, study areas, presumptions, and the types and sources of data employed [12].

Analytical equation-based approaches [13] are frequently used to estimate LULC changes. Additionally, there are statistical models [14]. Markov models [15], multi-agent models [16], expert system models [17], cellular models [18],

and hybrid models [19]. Cellular and agent-based models, or a hybrid model based on these two types, are now the most often employed models in LULCC monitoring and prediction [20]-[22].

Combining the concepts of Markov chains and cellular automata (CA-Markov) results in a hybrid model. To effectively simulate the spatial variation in a complex system, this model combines the benefits of the long-term predictions of the Markov model with the capabilities of the Cellular Automata (CA) model [23].

Benefits of the CA-Markov model for LULCC research include its capacity for dynamic simulation, high data efficiency, scarcity, easy calibration, and the ability to simulate a variety of land cover types and intricate patterns [24], [25]. The CA-Markov model has been widely utilized by scholars to track and predict changes in landscapes and land use [26], [27], and [28].

This research evaluates LULC from 1986 to 2020 and projects into the future (2030) using geospatial analysis on the state lands of Cape Coast, Ghana. This study provides decision-makers with important data for sustainable growth and comprehensive local environmental change, in addition to helpful planning and management information.

II. STUDY AREA

The study was performed for the Cape Coast Metropolitan Assembly (CCMA), which is abutted by the following districts: Twifu Hemang Lower Denkyira on the north, Abura Asebu Kwamankesse on the east, the Gulf of Guinea on the south, and Komenda Edina Eguafu Abirim on the west. It is geographically located between longitudes 001° 13'W and 001° 22'W and latitudes 005°05'N and 005°15'N, with an approximate area coverage of 122 km².

With the batholith as the dominant feature, it is characterised by an undulating landscape with a relatively high temperature. Saturated with most of Ghana's leading second-cycle educational institutions—a public university and a technical university—its literacy rate is 74.1% [29]. Fig. 1 represents the district map of the CCMA.

III. DATA COLLECTION

LULC data for the CCMA were gathered from the United States Geological Survey (USGS), as shown in Table I. These datasets were classified to perform LULC mapping between distinct LULC classes such as built-up areas, water bodies, and vegetation, as described in Table II.

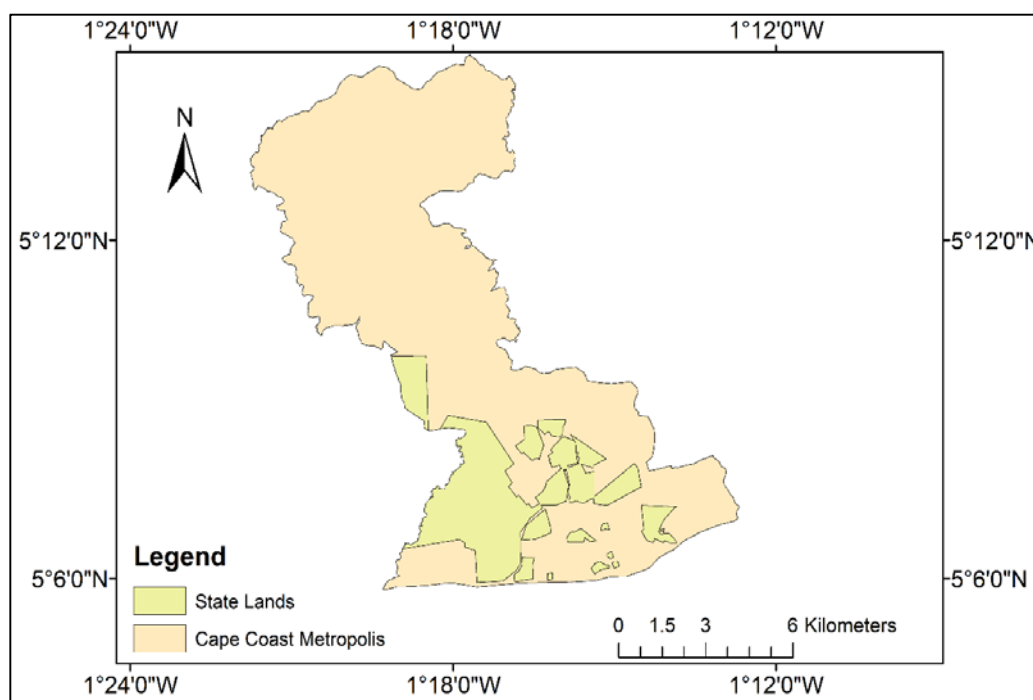


Fig. 1 District Map of Cape Coast Metropolitan Assembly

TABLE I
 SATELLITE DATA SOURCE

Satellite images	Date Acquired	Resolution/Pixel Size (m)	Image Quality	Land Cover (%)	Cloud Cover (%)	Number of Bands
Landsat 4 TM	01-01-1986	30	9	9	0	7
Landsat 7 ETM+	01-15-2000	30	7	9	9	9
Landsat 7 ETM+	01-15-2010	30	9	9	9	9
Landsat 8 OLI TIRS	03-01-2020	30	9	9	3.82	11

IV. METHODOLOGY

The study procedures include image pre-processing, image classification, change prediction, and validation. Fig. 2 illustrates a flow chart that summarises these procedures. Pre-processing is essential for assessing LULC change since errors due to image sensors, atmospheric effects, and Earth's curvature might produce inaccurate findings if they are not corrected [30].

A. Image Classification and Accuracy Assessment

Satellite images cover a wider area of spatial features, which are made possible through signals travelling to and from objects through the atmosphere to sensors onboard imaging platforms. The outcome images are therefore not without noise resulting from missed or incomplete, inconsistent, and false values, rendering images indistinguishable from originally captured objects as observed by [31]. For better results to be obtained from a satellite survey, radiometric and atmospheric corrections (quantitative outputs), geometric correction, and spatial sub-setting (qualitative outputs), generally referred to as pre-processing, must be done to ensure an image with better reflectance quality depicting true ground representation (geo-referenced data). The pre-processing technique was catered for in this study by the ENVI software. The processing of pre-processed images was performed in Arc Map, where various thematic layers from the various bands were clipped to form a land cover mosaic for detail classification. Image pixels were categorised into numerous LULC classes based on similar or differing spectral reflectance based on trained samples [32].

The trained samples for this study were based on mapped data from Google Earth and online imagery from Global Mapper. High-quality change detection findings were ensured by uniformly and randomly scattering sixty ground truth data points over the area. 30 training points were used to classify the 2020 image, together with local information and Google Earth photos. After that, the remaining thirty points were used to assess how well the image was classified. Using a supervised classification approach based on maximum likelihood, the research region was split into three (3) land use categories: (1) built-up; (2) vegetation; and (3) water.

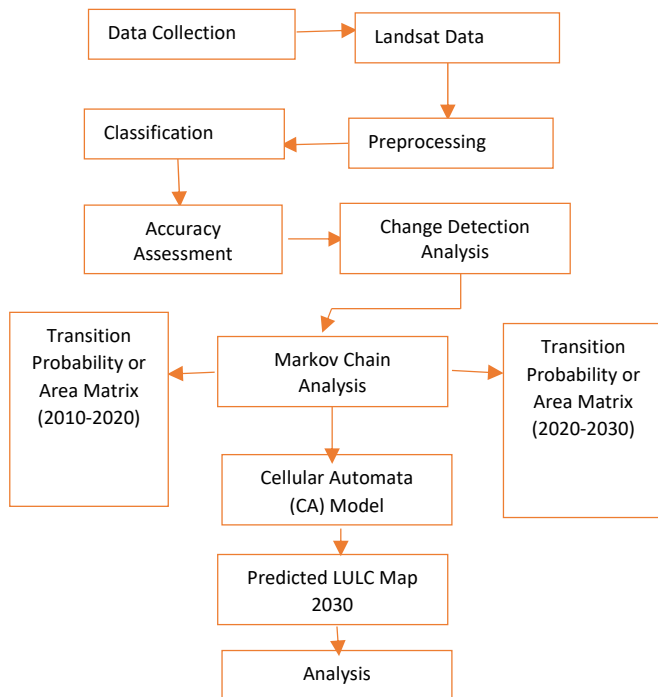


Fig. 2 Schematic Workflow for Methodology

TABLE II
 LAND USE CLASSES

Land use Class	Feature
Vegetation	Any land having woody plants, plantations, shrubs, grassland and cropped land.
Built-up	All of the land that has been developed, including social amenities like roads and highways for transportation, built-up regions and undeveloped terrain.
In land Water	These are areas of land that are submerged or covered in water for a portion of the year (for example, Lagoon).

B. Change Detection Analysis

To evaluate the LULCC that has occurred for the thirty-four-year period (1986–2020), the study used post-classification change detection. The three-time periods (1986–2000, 2000–2010, and 2010–2020) yielded the following results: change maps, contributions to the net change by land-cover type, and net gains or losses in hectares (ha) and percentages (%) for each land-cover category. Equation (1), as adopted in [32], was used to determine the yearly rate of LULC change.

$$R = \frac{100 \times (A_2 - A_1)}{A_1} \times \frac{1}{t_2 - t_1} \quad (1)$$

where R is the rate of LULC change A₁ and A₂ are the area of the first epoch and second epoch respectively.

C. Modelling and Predicting LULCC

In modelling and predicting LULCC, the study adopted the use of Markov Chain (MC) analysis and Cellular Automata (CA-Markov) to predict LULCC. The Markov model, according to [31], is used to forecast LULC change through a stochastic approach where a given class changes over time. Land-use change(s) over some time can be mathematically expressed as a matrix in a state. In a state, the transition probability matrix is determined in (2):

$$S(t, t + 1) = P_{ij} \times S(t) \quad (2)$$

where S(t) represents the system's status at time (t), S(t+1) represents the system's status at time (t+1), and P_{ij} represents the transition probability, which is determined in (3):

$$P_{ij} = \begin{bmatrix} P_{11} & \dots & P_{1n} \\ \vdots & \ddots & \vdots \\ P_{n1} & \dots & P_{nn} \end{bmatrix}, (0 \leq P_{ij} \leq 1) \quad (3)$$

where P is the transition probability. P_{ij} is the probability of converting from the present state (i) to another state (j) in time (t+1), and P_n is the state probability at any time.

To project land use trends by 2030, a transition probability matrix was developed for 2010–2020. A cross-tabulation of two periods using land use photos was used to build this matrix. According to [33], the prediction model can replicate spatial dynamics by considering the state of nearby cells at a particular moment in time.

The condition of neighbouring cells across time and the specified transition matrix are employed in CA to update each cell in the landscape. Spatial-temporal dynamics combine with

CA dynamics to mimic changes in two-dimensional space [34]. The CA-Markov model used to estimate LULC dynamics for the 2030-year prediction was verified to ensure the model's optimal performance. This was done by predicting the 2020 LULCC and comparing it with the actual 2020 LULCC. The results were analysed for accuracy performance using the Kappa Index of Agreement (KIA) for the actual and predicted image for the 2020 year and were determined to be within the range for the approved classification accuracy range.

C. Model Validation

The model was evaluated for validity by employing the Kappa Index after producing a simulated map. This Kappa statistic is distinct from typical Kappa statistics. It splits the validation into numerous components, each with a distinct form of Kappa and the statistics that go with it, such as K-no information, K-location, K-standard, and so on. [33]. After achieving successful Kappa values, the CA-Markov model was used to simulate the LULC change maps for 2020 and 2030. According to [34], (4)-(6) give the summary statistics for the Kappa fluctuations:

$$K_{no} = (M_{(m)}N_{(n)}) / (P_{(p)} - N_{(n)}) \quad (4)$$

$$K_{location} = (M_{(m)}N_{(n)}) / (P_{(p)} - N_{(n)}) \quad (5)$$

$$K_{standard} = (M_{(m)}N_{(n)}) / (P_{(p)} - N_{(n)}) \quad (6)$$

where N(n) denotes no information, M(m) denotes medium grid cell-level information, and P(p) denotes perfect grid cell-level information across the landscape.

TABLE III
 CA-MARKOV CHAIN MODEL STATISTICAL VALIDATION-2020

Statistics	Value (%)
K_no	84.44
K_location	93.96
K_standard	78.89

V. RESULTS AND DISCUSSION

A. Classification

LULC classifications for 1986, 2000, 2010, and 2020 were performed on the acquired images with three land cover types based on supervised classification and the FAO classification scheme. These include:

- i. built-up areas (settlement and bare soil because of their close reflectance value);
- ii. vegetation (shrubs, grassland, open woodland, agricultural or farmland, etc.); and
- iii. inland water (streams, lagoons, etc.).

An accuracy assessment was performed for 2020, and the results showed an overall accuracy of approximately 85% and a Kappa coefficient of 0.80, indicating substantial agreement. As a result, there was very little class misunderstanding, and the land cover classes were designated.

Four land cover maps were generated. The land cover map

for 1986 was mainly dominated by vegetation (Fig. 3 and Table IV), with the area and percentage of cover for built-up areas, vegetation, and inland water being 3.75 km² (17.11%), 17.63 km² (80.43%), and 0.54 km² (2.46%), respectively.

The total land size spanning the study area derived from the shape file for the state land holdings within the Metropolis was found to be approximately 22 km² (21.92 km²).

LULC of the entire state lands in CCMA was still dominated by vegetation as of 2000 (Fig. 4), with a minimum growth in built-up areas. The coverage of vegetation was 12.25 km², built-up areas were 9.19 km² and inland waters were 0.48 km². These represent 55.90%, 41.93%, and 0.48% of the total land area, respectively (Table IV).

The 2010 and 2020 land cover maps also showed that vegetation decreased drastically, with 8.23 km² representing 37.55% of the land area for 2010 and 4.95 km² representing 22.58% for 2020. Built-up (bare land) and concrete surfaces continued to grow in number, occupying 13.17 km² (60.09%) in 2010 and 16.33 km² (74.5%) in 2020 of the total state lands of the Metropolis. Equally for the said two years in succession, inland water appreciated by 0.52 km² (2.36%) and 0.64 km² (2.92%), as shown in Figs. 4 and 5 and Table IV.

The regional statistical breakdown of the urban population of Ghana has always placed the Central Region in the third position, from independence until the last census year. This observation can equally account for the findings of the spatial analysis and the results in Table IV, and upon inference, similar reasons can be attributed to why the State lands in the Metropolis is losing its vegetative cover to rapid urban development.

B. Change Detection Analysis

Table V presents changes in land cover types over various time intervals (1986-2000, 2000-2010, 2010-2020, and 1986-2020) for built-up areas, vegetation, and water bodies. It was seen that there was an increase in built-up areas over all intervals, with gains ranging from 3.98 km² to 10.36 km² and the rate of change was 9.8 (1986-2020)

The percentage change also demonstrates consistent growth, ranging from 12.58% to 57.39%. This trend suggests urbanization and infrastructure development. While it indicates economic growth and increased human activity, it also implies potential environmental impacts such as habitat loss, increased impervious surfaces leading to drainage issues, and higher energy consumption due to urban heat island effects.

Vegetation shows a consistent loss across all intervals, ranging from 2.18 km² to 5.38 km² and a rate of change of 5.14 (1986-2020). The percentage change in vegetation loss ranges from 12.68% to 57.85%. The decline in vegetation could indicate deforestation, agricultural expansion, or the degradation of natural habitats. It raises concerns about biodiversity loss, soil erosion, reduced carbon sequestration, and impacts on local climates and ecosystems.

Water bodies show fluctuating changes, with losses and gains observed across different intervals. The overall trend indicates a slight increase in water bodies over the entire

period (1986–2020). Changes in water bodies can be influenced by various factors, such as climate change, land use changes, and hydrological alterations.

While a slight increase in water bodies may seem positive, it is essential to consider the quality and ecological health of these bodies, as well as potential implications for flood risk and water resource management. Continuous monitoring of land cover changes using RS and GIS technologies is crucial for assessing trends, identifying hotspots of change, and informing decision-making processes.

Long-term planning that considers the ecological, social, and economic implications of land cover changes is essential for sustainable development and biodiversity conservation.

By analysing the trends and drivers behind the changes in

built-up areas, vegetation, and water bodies as depicted in Table V, stakeholders can better understand the evolving landscape and implement strategies to promote sustainable land use practices, protect ecosystems, and address the challenges posed by land cover transformations.

TABLE IV
 CHANGES IN LAND COVER (1986-2020)

Land Cover Class	1986 Area km ²	1986 Area %	2000 Area km ²	2000 Area %	2010 Area km ²	2010 Area %	2020 Area km ²	2020 Area %
Built-Up	3.75	17.11	9.19	41.93	13.17	60.09	16.33	74.50
Vegetation	17.63	80.43	12.25	55.90	8.23	37.55	4.95	22.58
Water	0.54	2.46	0.48	0.48	0.52	2.36	0.64	2.92
Total	21.92	100	21.92	100	21.92	100	21.92	100

TABLE V
 CHANGE DETECTION

Year Interval	1986 to 2000			2000 to 2010			2010 to 2020			1986 to 2020		
LULC considered	Area (km ²)	%Change	Rate	Area (km ²)	% Change	Rate	Area (km ²)	%Change	Rate	Area (km ²)	%Change	Rate
Built-up Areas	5.44 (gain)	24.82 (gain)	10.36 (gain)	3.98 (gain)	18.16 (gain)	4.91 (gain)	3.16 (gain)	14.41 (gain)	2.40 (gain)	12.58 (gain)	57.39 (gain)	9.8 (gain)
Vegetation	5.38 (loss)	24.53 (loss)	2.18 (loss)	4.021 (loss)	8.35 (loss)	3.28 (loss)	3.28 (loss)	14.97 (loss)	3.99 (loss)	12.68 (loss)	57.85 (loss)	5.14 (loss)
In-land Water	0.06 (loss)	0.29 (loss)	0.79 (loss)	0.04 (gain)	0.19 (gain)	0.83 (gain)	0.12 (gain)	0.56 (gain)	2.31 (gain)	0.10 (gain)	0.46 (gain)	0.54 (gain)

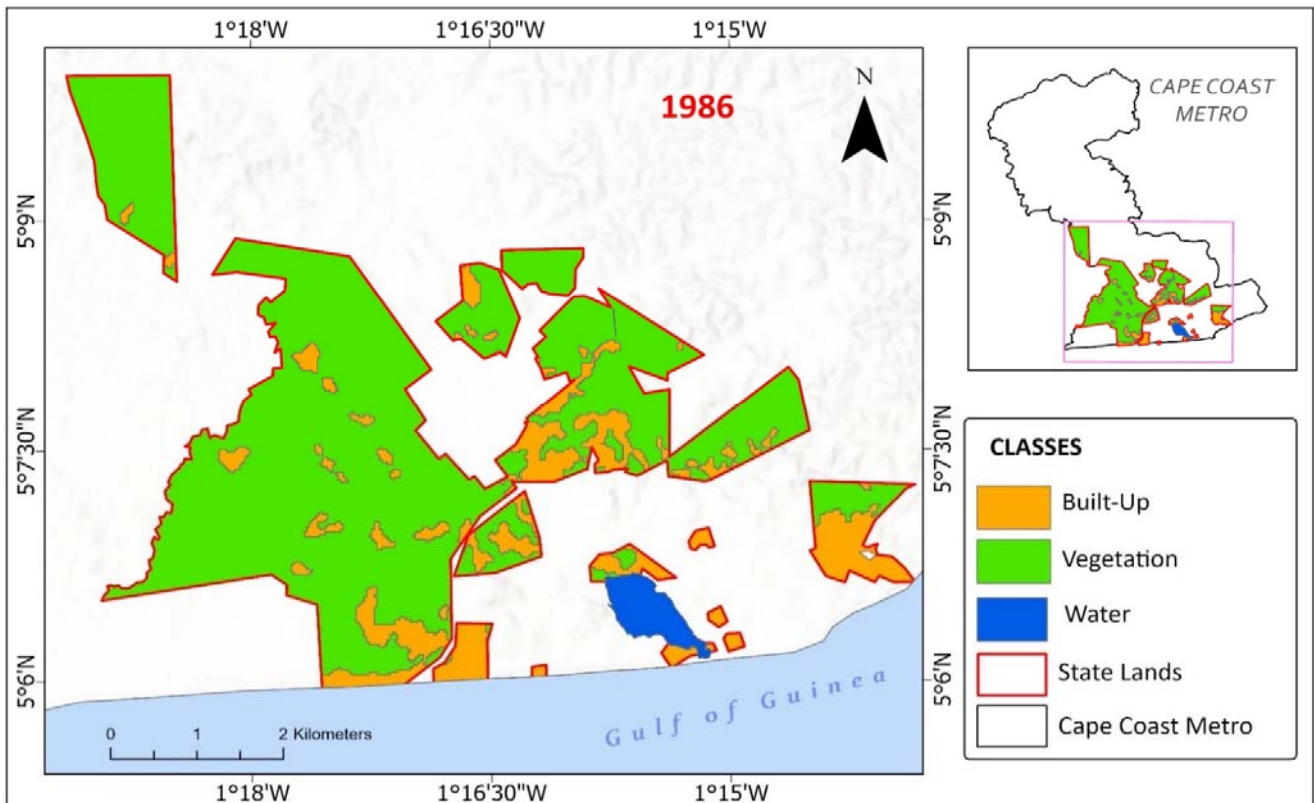


Fig. 3 LULC Map for 1986

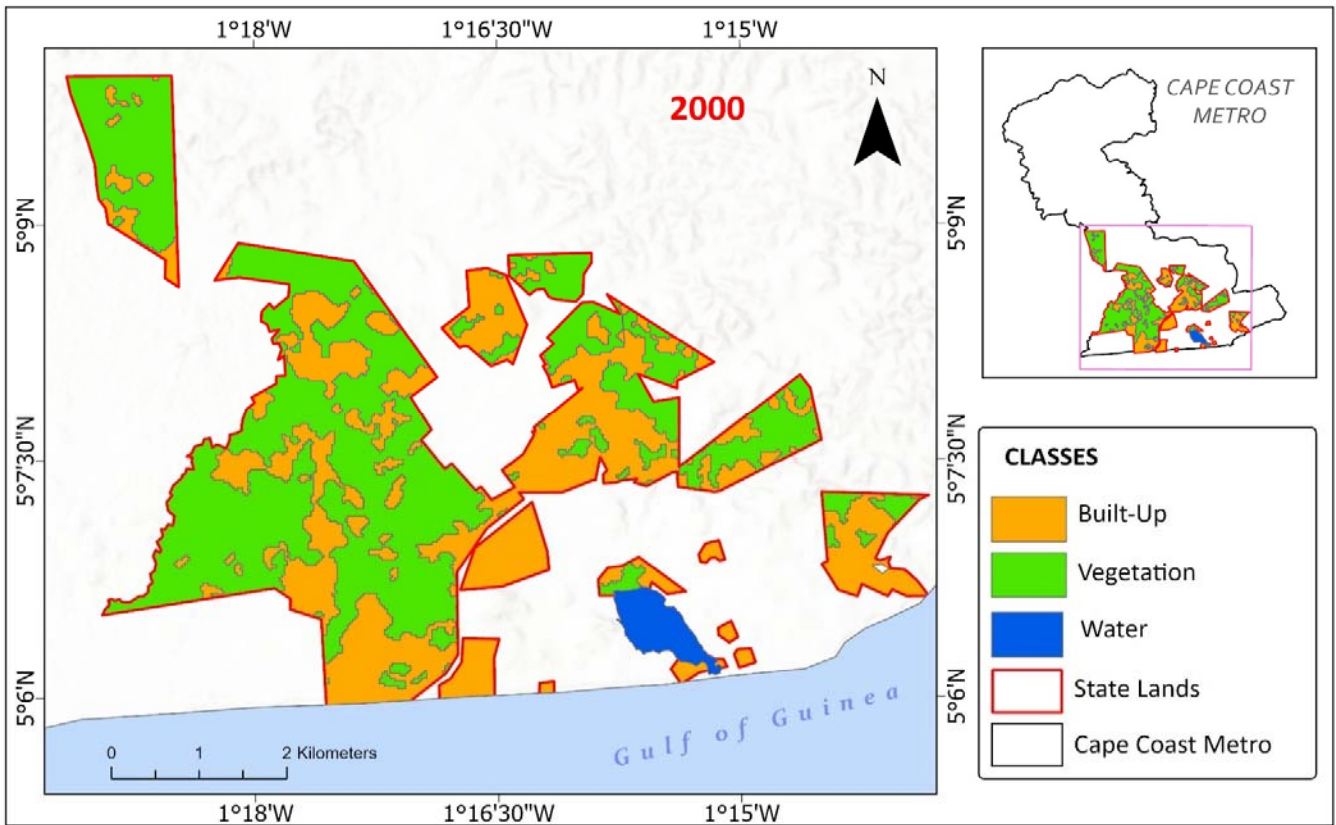


Fig. 4 LULC Map for 2000

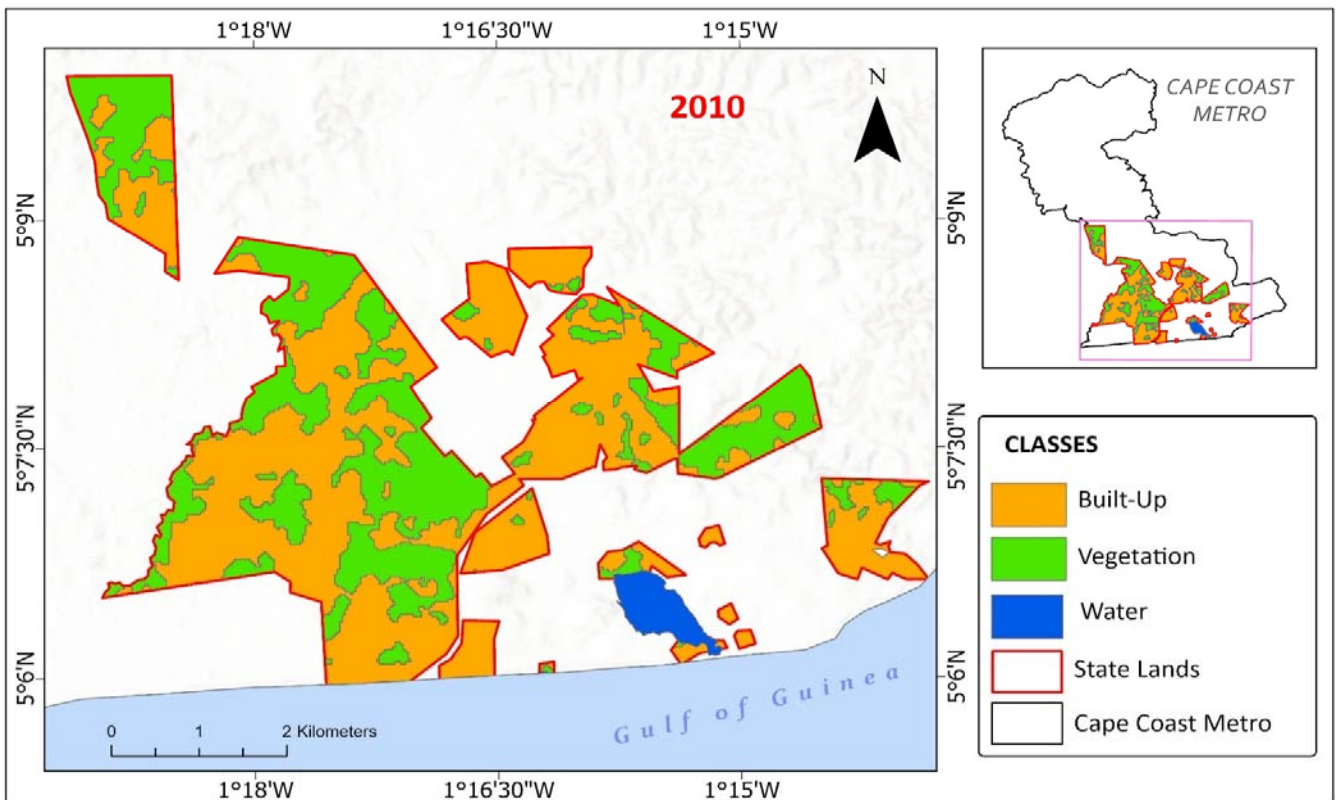


Fig. 5 LULC Map for 2010

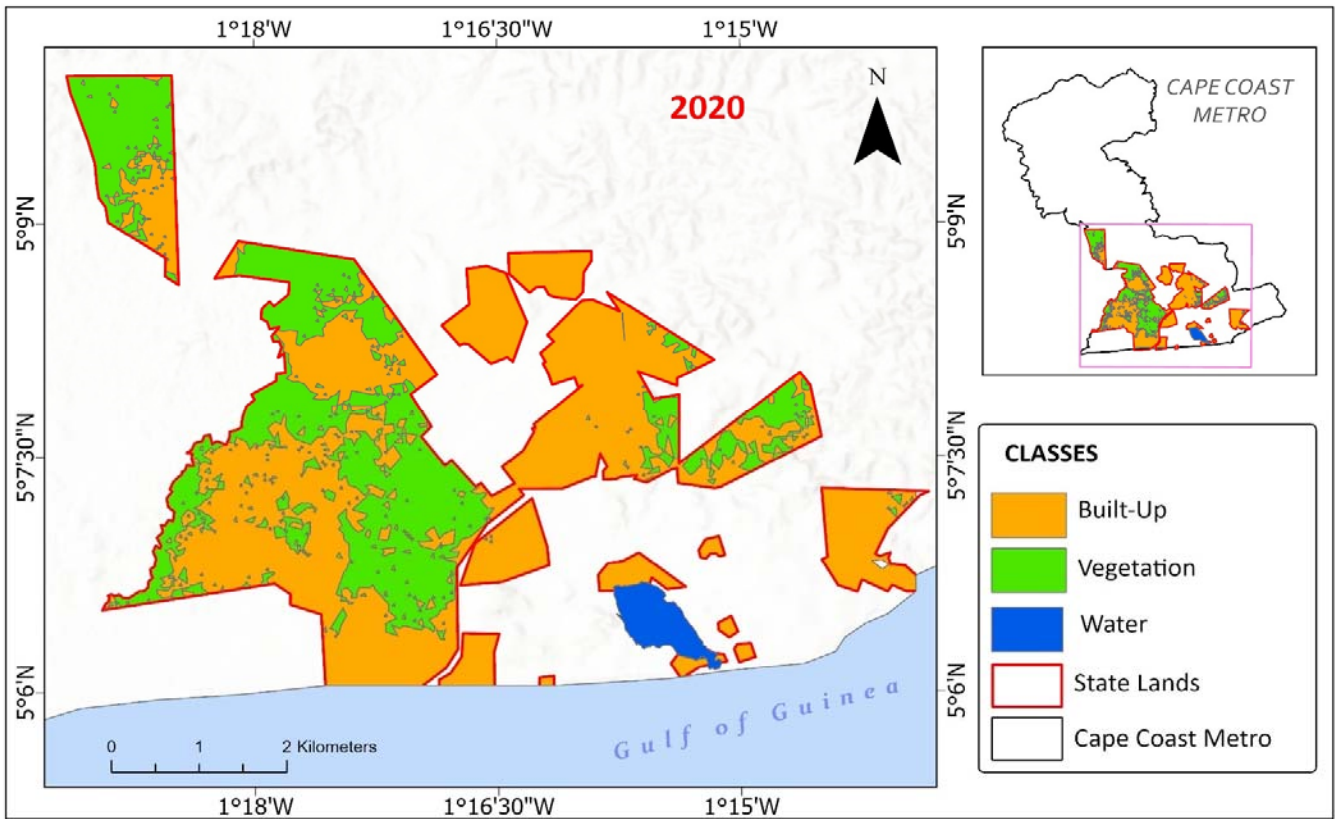


Fig. 6 LULC Map for 2020

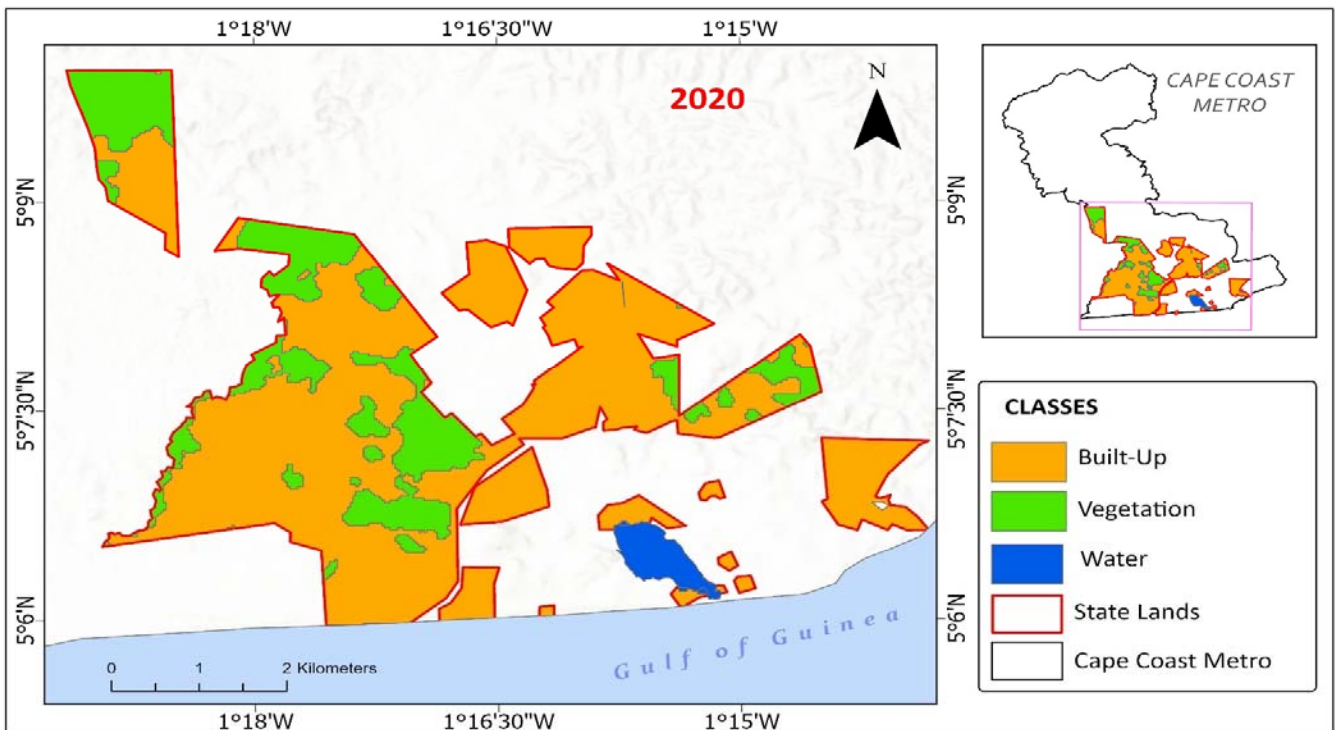


Fig. 7 Predicted LULC Map for 2020

B. Land Cover Simulation and Prediction for 2030

Before applying the CA-Markov model to estimate the

LULC map of 2030, the LULC map of 2020 was simulated. The LULC maps of 2000 and 2010 were used to forecast the

LULC map for 2020. The simulated land use areas were linked to the actual land use of the specified state lands in the Cape Coast metropolis to validate or assess the accuracy of the LULC forecast given by the CA-Markov model.

The model's performance was evaluated using the Kappa index (Table III). Table VI compares actual and simulated LULC 2020 maps. The simulated LULC map shows that built-up regions are slightly overestimated, while vegetation and water areas are significantly underestimated. However, these findings, as shown in Table VI, indicate a striking similarity between the actual and predicted maps for 2020.

All LULC classifications showed a good range of agreement across the two maps' areas covered, as evidenced in Table III, where the overall accuracy (K_{no}) is 0.8444, the location quotient ($K_{locations}$) is 0.9396, and the quantity allocation ($K_{standard}$) is 0.7889, which is above 0.75 and indicates a satisfactory level of accuracy. Figs. 6 and 7 depict

the actual and predicted LULC maps for 2020, respectively.

TABLE VI
 COMPARISON OF ACTUAL AND PREDICTED LULC 2020

Land Cover Class	Predicted Area (km ²)	%	Observed /Actual Area (km ²)	%
Built-Up	16.87	79.96	16.33	74.50
Vegetation	4.43	20.21	4.95	22.58
Inland water	0.62	2.83	0.64	2.92
Total	21.92	100	21.92	100

TABLE VII
 PREDICTED AREA AND PERCENTAGE COVERAGE FOR 2030

Land Cover Class	Area (km ²)	Area (%)
Built-up	17.64	80.47
Vegetation	3.60	16.43
Inland water	0.68	3.10
Total	21.92	100

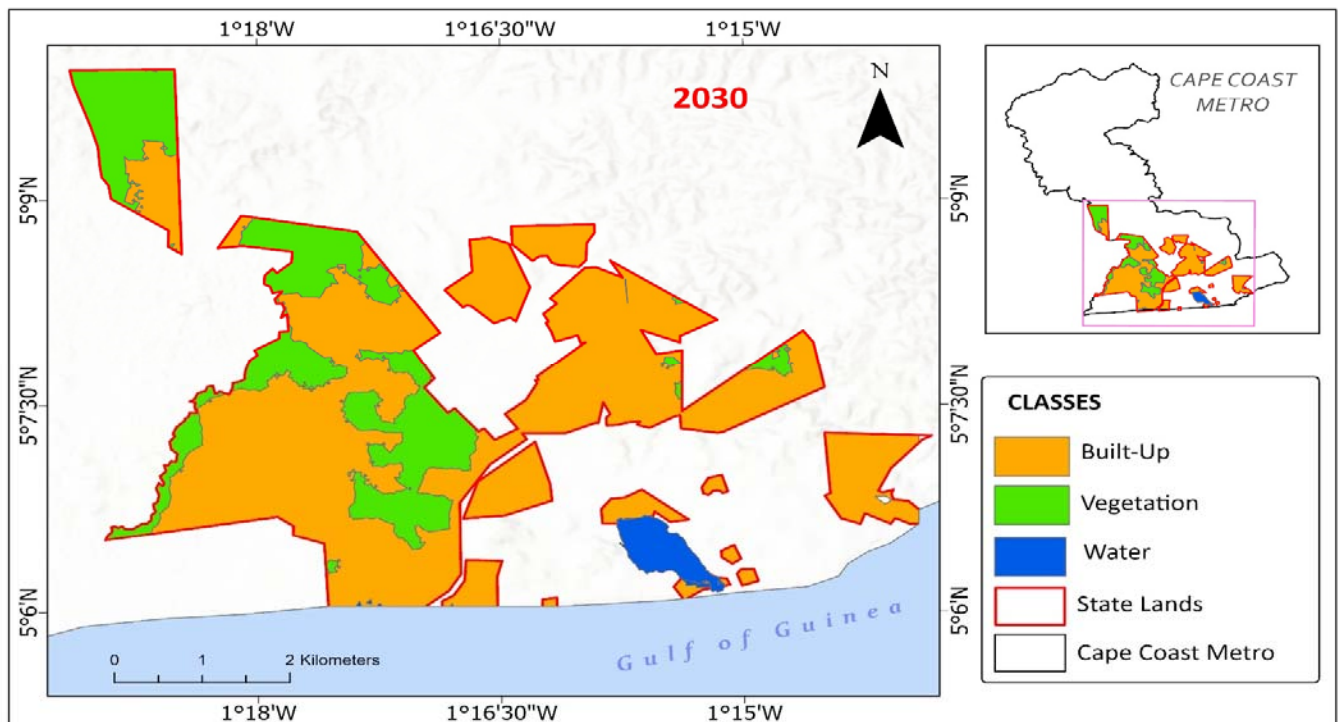


Fig. 8 Predicted LULC Map 2030

TABLE VIII
 PROPORTION UNITS GAINED AND/OR LOST FOR THE PROJECTED 2030

Land Cover Class	2020-2030	
	Area (km ²)	Percentage (%)
Built-up	1.31 (gain)	5.97 (gain)
Vegetation	1.35 (loss)	6.15 (loss)
Inland water	0.04 (gain)	0.18 (gain)

The model was put into operation after the validation to predict the LULC map for 2030 using the land use map of the 2010-2020 transition area matrices and the 2020 transition potential map. This 10-year LULC is based on how well the model performed for the 2020 predicted LULC map (Fig. 7). Fig. 8 depicts the expected LULC Map of state lands in the

Cape Coast Metropolis by 2030.

Table VII shows a quantification comparison between the LULC map for 2020 and predicted 2030. By extension, Table VIII presents the anticipated proportion of units of gain and or loss for the projected 2030-year period. In a similar trend to the discussion for Table 8, built-up will gain an area of 1.31 km² which translates a 0.13 km² (34.59 acres or 13.99 hectares) every year till 2030.

Vegetation will equally lose an area of 1.35 km² translating a 0.14 km² (34.59 acres or 13.99 hectares) annually till 2030 with a negligible gain of 0.04 km² for inland water for the same period. For 2030, the various LULC classes are expected to increase by 1.31 km², and 0.04 km² and lose out by 1.35

km² respectively for built-up, water and vegetation. Percentage data for the aforementioned also reveal 5.97% and 0.18% gains for built-up and water, respectively, and a 6.15% loss in vegetation, as seen in Table VIII. By this projection, sound planning and developmental policies can be formulated to ensure sustainability for both present and future generations.

VI. CONCLUSION

The importance of LULC in the State Lands of the CCMA of Ghana has been illustrated by this study, which shows how important it is to provide relevant data on time for decisions on the loss or reduction of vegetation in forests and the burgeoning built-up areas. It has been feasible to find out specifics regarding the size and kind of each LULC while showcasing LULC modelling in the research region with the help of the techniques employed for obtaining LULC maps (1986, 2000, 2010, 2020, and 2030).

The results of this study generally indicate that the classification of RS images (supervised) is a powerful method for obtaining appropriate LULC maps. It was determined that the CA-Markov model's predicting ability was adequate. A comprehensive study on environmental change and sustainable development at the local, national, regional, and continental levels can greatly benefit from the knowledge provided by LULC investigations.

Decision-makers can utilise these research findings to help with planning and management. Under the CCMA years of 1986–2000, 2000–2010, and 2010–2020, the research focused on the following issues: increasing built-up areas, decreasing agricultural land, and forest loss (deforestation and degradation). The research area's overall LULC pattern comprised a decrease in vegetation, an increase in built-up land, and a loss of woodland. Because the water bodies in the research region are significant national assets and are properly protected, they have remained rather stable. Over the last 34 years, the predominant LULC trend has been the shift from forest and agricultural land to built-up land.

The main trends of past LULC transformations in the research region were identified by this study, and they were suggested for potential LULC transition processes in the future. The investigation confirmed that the CA-Markov model is a practical method for LULC prediction. As such, the CA-Markov model is essential to the creation and formulation of LULC policies. By analysing the trends and drivers behind the changes in built-up areas, vegetation, and water bodies as depicted in Table V, stakeholders can better understand the evolving landscape and implement strategies to promote sustainable land use practices, protect ecosystems, and address the challenges posed by land cover transformations.

REFERENCES

[1] Uttara, S., Bhuvandas, N. and Aggarwal, V. (2012), "Impacts of Urbanization on Environment", *International Journal of Research in Engineering and Applied Sciences*, Vol. (2), pp. 1637-1645.
[2] GSS (Ghana Statistical Survey), 2010 Population and Housing Census, 2012.
[3] Nsiah-Gyabaah K. (2010), "Urbanization Processes-Environmental and Health effects in Africa", Panel Contribution to the PERN Cyber

seminar on Urban Spatial Expansion. Principal, Sunyani Polytechnic, Ghana.
[4] Forkuor, D. (2010), "Land allocation and its effects on the spatial planning and development of Kumasi Metropolis", Doctor of Philosophy (PhD) Thesis, Kwame Nkrumah University of Science and Technology, Faculty of Social Sciences, Kumasi.
[5] Goswami, M., Ravishankar, C., Nautiyal, S. and Schaldach, R. (2019), "Integrated Landscape Modelling in India: Evaluating the Scope for Micro-Level Spatial Analysis over Temporal Scale", In *Tropical Ecosystems: Structure, Functions and Challenges in the Face of Global Change*, pp. 289–315. Springer, Singapore.
[6] Kleemann, J., Baysal, G., Bulley, H.N. and Fürst, C. (2017), "Assessing Driving Forces of Land Use and Land Cover Change by a Mixed-Method Approach in North-Eastern Ghana", *West Africa, Journal of Environmental Management*, Vol. (196), pp. 411–442.
[7] Acheampong, M., Yu.Q., Enomah, L.D., Anchang, J. and Eduful, M. (2018), "Land Use/Cover Change in Ghana's Oil City: Assessing the Impact of Neoliberal Economic Policies and Implications for Sustainable Development Goal Number One—A Remote Sensing and GIS Approach", *Land Use Policy*, Vol. (73), pp. 373–384.
[8] Pervez, W., Uddin, V., Khan, S.A. and Khan, J.A. (2016), "Satellite-Based Land Use Mapping: Comparative Analysis of Landsat-8, Advanced Land Imager and Big Data Hyperion Imagery", *Journal of Applied Remote Sensing*, Vol. (10).
[9] Singh, P., Kikon, N. and Verma, P. (2017), "Impact of Land Use Change and Urbanization on Urban Heat Island in Lucknow City, Central India, A Remote Sensing-Based Estimate", *Sustainable Cities and Society*, Vol. (32), pp. 100–114.
[10] Panwar, S. And Malik, D.S. (2017), "Evaluating Land Use/ Land Cover Change Dynamics in Bhimtal Lake Catchment Area, Using Remote Sensing and GIS Techniques", *Journal of Remote Sensing And GIS*, Vol. (6), No. (199), 2 pp.
[11] Liping, C., Yujun, S. and Saeed, S. (2018), "Monitoring and Predicting Land Use and Land Cover Changes Using Remote Sensing and GIS Techniques", A Case Study of a Hilly Area, Jiangle, China, *Plos ONE*, Vol. (13), No. (7), pp. 200-493.
[12] Michetti, M. And Zampieri, M. (2014), "Climate-Human- Land Interactions: A Review of Major Modelling Approaches", *Land*, Vol. (3) No. (3), pp. 793–833. DOI:10.3390/Land3030793.
[13] Shamsi, S.R.F. (2010), "Integrating Linear Programming and Analytical Hierarchical Processing in Raster GIS to Optimize Land Use Pattern at Watershed Level", *Journal of Applied Sciences and Environmental Management*, Vol. (14), No. (2), pp. 81–84.
[14] Hyandye, C. (2015), "A Markovian and Cellular Automata Land-Use Change Predictive Model of the Usungu Catchment", *International Journal of Remote Sensing*, pp. 64–81.
[15] Koranteng, A., Adu-Poku, I., Donkor, E. and Zawila-Niedzwiecki, T. (2020), "Geospatial Assessment of Land Use and Land Cover Dynamics in the Mid-Zone of Ghana", *Folia Forestalia Polonica*, Vol. (62) No. (4), pp.288–305. doi:https://doi.org/10.2478/ffp-2020-0028.
[16] Ralha, C.G., Abreu, C.G., Coelho, C.G.C., Zaghetto, A., Macchiavello, B. and Machado, R.B. (2013), "A Multiagent Model System for Land-Use Change Simulation", *Remote Sensing of Environment*, Vol. (42), pp. 30–46.
[17] Stefanov, W.L., Ramsey, M.S. and Christensen, P.R. (2001), "Monitoring Urban Land Cover Change: An Expert System Approach to Land Cover Classification of Semiarid to Arid Urban Centers", *Remote Sensing of Environment*, Vol. (77), No. (2), pp. 173–185.
[18] Singh, S.K., Mustak, S., Srivastava, P.K., Szabó, S. and Islam, T. (2015), "Predicting Spatial and Decadal LULC Changes Through Cellular Automata Markov Chain Models Using Earth Observation Datasets and Geo-Information", *Environmental Processes*, Vol. (2), No. (1), pp. 61–78.
[19] Subedi, P., Subedi, K. and Thapa, B. (2013), "Application of A Hybrid Cellular Automaton-Markov (CA-Markov) Model in Land-Use Change Prediction: A Case Study of Saddle Creek Drainage Basin, Florida", *Science and Education*, Vol. (1), No. (6), pp. 126–132.
[20] Sohl, T.L. and Claggett, P.R. (2013), "Clarity Versus Complexity: Land-Use Modelling as A Practical Tool for Decision-Makers", *Journal of Environmental Management*, Vol. (129), pp. 235–243.
[21] Zhao, L. and Peng, Z.-R. (2012), "Land System: An Agent-Based Cellular Automata Model of Land Use Change Developed for Transportation Analysis", *Journal of Transport Geography*, Vol. (25), pp. 35–49.
[22] Stevens, D. and Dragičević, S. (2007), "A GIS-Based Irregular Cellular

- Automata Model of Land-Use Change”, *Environment and Planning B: Urban Analytics and City Science*, Vol. (34), No. (4), pp. 708–724.
- [23] He, J., Li, X., Yao, Y., Hong, Y. and Jinbao, Z. (2018), “Mining Transition Rules of Cellular Automata for Simulating Urban Expansion by Using the Deep Learning Techniques”, *International Journal of Geographical Information Science*, Vol. (32), No. (10), pp. 2076–2097.
- [24] Hyandye, C. and Martz, L.W. (2017), “A Markovian and Cellular Automata Land-Use Change Predictive Model of the Usangu Catchment”, *International Journal of Remote Sensing*, Vol. (38), No. (1), pp. 64–81.
- [25] Memarian, H., Balasundram, S.K., Talib, J.B., Sung, C.T.B., Sood, A.M. and Abbaspour, K. (2012), “Validation Of CA-Markov for Simulation of Land Use and Cover Change in the Langat Basin, Malaysia”, *Journal of Geographic Information System*, Vol. (4) No. (6), pp. 542–554.
- [26] Etemadi, H., Smoak, J.M. and Karami, J. (2018), “Land Use Change Assessment in Coastal Mangrove Forests of Iran Utilizing Satellite Imagery and CA-Markov Algorithms to Monitor and Predict Future Change”, *Environmental Earth Sciences*, Vol. (77) No. (5), 208pp.
- [27] Rimal, B., Zhang, L., Keshtkar, H., Wang, N. and Lin, Y. (2017), “Monitoring and Modeling of Spatiotemporal Urban Expansion and Land-Use/Land-Cover Change Using Integrated Markov Chain Cellular Automata Model”, *ISPRS International Journal of Geo-Information*, Vol. (6), No. (9), 288pp.
- [28] Mansour, S., Al-Belushi, M. and Al-Awadhi, T. (2020), “Monitoring Land Use and Land Cover Changes in The Mountainous Cities of Oman Using GIS and Camarkov Modelling Techniques”, “*Land Use Policy*, 91”, DOI: 10.1016/J.Landusepol.2019.104414
- [29] Parsa, V.A., Yavari, A. and Nejadi, A. (2016), “Spatio-Temporal Analysis of Land Use/Land Cover Pattern Changes in Arasbaran Biosphere Reserve: Iran”, *Modeling Earth Systems and Environment*, Vol. (2), No. (4), pp.1–13.
- [30] Chatterjee, S., Ghosh, Dey, N. (2016), “Forest type classification: A Hybrid NN-GA model-based approach”, In *Information Systems Design and Intelligent Applications*, pp. 227–236.
- [31] Lilles and., T. M. and R. W. (2000), “Remote Sensing and Image interpretation”, John Wiley and Sons, New York.
- [32] Hamad, R. Balzter, H. and Kolo, K. (2018), “Predicting land use/land cover changes using a CA-Markov model under two different scenarios, *Sustainability*, Vol. (10), No. (10), pp. 1-23.
- [33] Abdulrahman, A. I. and Ameen, S.A. (2020), “Predicting Land Use and Land Cover Spatiotemporal Changes Utilizing CA-Markov Model in Duhok District between 1999 and 2033”, *Academic Journal of Nawroz University*, vol. 9, no. 4, pp.71. doi: <https://doi.org/10.25007/ajnu.v9n4a892>.
- [34] Omar, N. Q., Ahamad, M. S. S., Wan Hussin, W. M. A., Samat, N. and Binti Ahmad, S. Z. (2013), “Markov CA, Multi Regression, and Multiple Decision Making for Modelling Historical Changes in Kirkuk City, Iraq”, *Journal of the Indian Society of Remote Sensing*, Vol. (42), No. (1), 2013, pp.165–178.doi: <https://doi.org/10.1007/s12524-013-0311-2>.